ACCOUNTS
of chemical research

The Chemistry of the Sulfur–Gold Interface: In Search of a Unified Model

EVANGELINA PENSA,[†] EMILIANO CORTÉS,[†] GASTÓN CORTHEY,[†] PILAR CARRO,[§] CAROLINA VERICAT,[†] MARIANO H. FONTICELLI,[†] GUILLERMO BENÍTEZ,[†] ALDO A. RUBERT,[†] AND ROBERTO C. SALVAREZZA*,[†]

[†]*Instituto de Investigaciones Fisicoquímicas Teóricas y Aplicadas (INIFTA), Universidad Nacional de La Plata - CONICET, Sucursal 4 Casilla de Correo 16 (1900) La Plata, Argentina, and* [§]*Departamento de Química Física, Instituto de Materiales y Nanotecnología, Universidad de La Laguna, Tenerife, Spain*

RECEIVED ON OCTOBER 11, 2011

CONSPECTUS

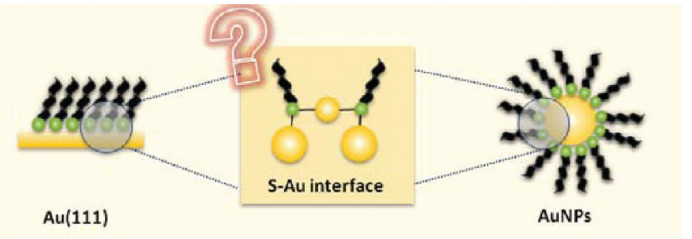

Over the last three decades, self-assembled molecular films on solid surfaces have attracted widespread interest as an intellectual and technological challenge to chemists, physicists, materials scientists, and biologists. A variety of technological applications of nanotechnology rely on the possibility of controlling topological, chemical, and functional features at the molecular level. Self-assembled monolayers (SAMs) composed of chemisorbed species represent fundamental building blocks for creating complex structures by a bottom-up approach. These materials take advantage of the flexibility of organic and supramolecular chemistry to generate synthetic surfaces with well-defined chemical and physical properties. These films already serve as structural or functional parts of sensors, biosensors, drug-delivery systems, molecular electronic devices, protecting capping for nanostructures, and coatings for corrosion protection and tribological applications.

Thiol SAMs on gold are the most popular molecular films because the resulting oxide-free, clean, flat surfaces can be easily modified both in the gas phase and in liquid media under ambient conditions. In particular, researchers have extensively studied SAMs on Au(111) because they serve as model systems to understand the basic aspects of the self-assembly of organic molecules on well-defined metal surfaces. Also, great interest has arisen in the surface structure of thiol-capped gold nanoparticles (AuNPs) because of simple synthesis methods that produce highly monodisperse particles with controllable size and a high surface/volume ratio. These features make AuNPs very attractive for technological applications in fields ranging from medicine to heterogeneous catalysis.

In many applications, the structure and chemistry of the sulfur–gold interface become crucial since they control the system properties. Therefore, many researchers have focused on understanding of the nature of this interface on both planar and nanoparticle thiol-covered surfaces. However, despite the considerable theoretical and experimental efforts made using various sophisticated techniques, the structure and chemical composition of the sulfur–gold interface at the atomic level remains elusive. In particular, the search for a unified model of the chemistry of the S–Au interface illustrates the difficulty of determining the surface chemistry at the nanoscale. This Account provides a state-of-the-art analysis of this problem and raises some questions that deserve further investigation.

Introduction

Self-assembled monolayers (SAMs) of thiols are key elements in nanoscience and nanotechnology. They have been used to link inorganic, organic, and biological materials to planar gold (Au) surfaces or gold nanoparticles (AuNPs).[1,2] SAMs on planar Au surfaces are widely used as building blocks for the fabrication of different type of devices by the bottom-up approach, while thiol-capped AuNPs have promising applications in biology, medicine, catalysis, photonics, and electronics.

Published on the Web 03/23/2012 www.pubs.acs.org/accounts
10.1021/ar200260p

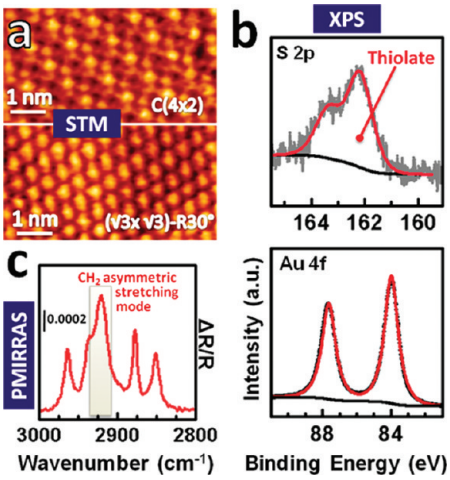

FIGURE 1. Surface characterization of typical alkanethiol SAMs on Au(111).

Sulfur (S) adsorption on Au is interesting because it is a usual impurity in thiols and can be formed on the surfaces by C–S bond scission. Also, S is a well-known poison in heterogeneous catalysis that could affect the efficiency of the promising oxide-supported AuNP catalysts. Finally, gold sulfide (AuS) nanoparticles have potential applications in nanomedicine and offer excellent prospects for probing biological systems.[3]

Despite the technological interest of these systems, the sulfur–metal interfacial chemistry remains one of the most controversial topics in nanoscience.[4] Here we present the state-of-the-art on a subject that challenges our ability to understand chemistry at the nanoscale.

The Thiolate–Au System: What is Known for Thiols on Au(111) and AuNPs

The initial stage of thiol chemisorption on Au(111) involves the formation of lying-down phases with molecules parallel to the substrate. Upon increase of the surface coverage, a transition from the lying-down to a standing-up configuration takes place, with the formation of domains of the dense and stable ($\sqrt{3} \times \sqrt{3}$)-R30° and c(4 × 2) thiol lattices, which can coexist on the substrate. Both have surface coverage $\theta = 0.33$ and nearest-neighbor thiol–thiol distances $d \approx 0.5$ nm (Figure 1a).[5,6] For short thiols, domains of more diluted lattices ($\theta < 0.33$) are also found.[5,7,8] Similar surface structures are formed in SAMs of aromatic thiols.[9,10] The chemisorption process induces strong changes in the substrate with the formation of vacancy islands of monatomic depth in the case of aliphatic thiols and of gold islands of monatomic height in most of the aromatic thiols.[9,11]

Irrespective of the aliphatic or aromatic character and surface structures, thiol molecules are chemisorbed on Au by a strong thiolate–Au bond (40–50 kcal mol^{-1}). This bond yields a S 2p X-ray photoelectron spectroscopy (XPS) signal at ~162 eV (Figure 1b), that is, at lower binding energy (BE) than bulk S (~164 eV). In some cases, a small amount of free thiol (~163 eV) is observed. The molecular backbone stabilizes the SAM via intermolecular forces (~6 kcal mol^{-1} for hexanethiol and ~12 kcal mol^{-1} for benzenethiol in a ($\sqrt{3} \times \sqrt{3}$)-R30° lattice).

An increment in the number of CH_2 units (n) in the hydrocarbon chain backbone markedly increases SAM order. Thus, the CH_2 asymmetric stretching mode observed by polarization modulation infrared reflection absorption spectroscopy (PMIRRAS) (Figure 1c) moves from ~2927 cm^{-1} ($n < 6$) to ~2917 cm^{-1} ($n > 12$)[12] as the number of gauche conformations around the C–C bonds decreases. Also the ($\sqrt{3} \times \sqrt{3}$)-R30°/c(4 × 2) coverage ratio in the SAMs increases with hydrocarbon chain length.[13,14] For crystalline-like SAMs, hydrocarbon chains adopt 30–40° tilt angles with respect to the surface normal.[6] As for aromatic thiol SAMs, their degree of order can be remarkably enhanced by increasing the number of benzene rings in the molecules,[15] which are also organized almost perpendicular to the Au(111) surface.[16] However, SAMs of large aromatic thiols exhibit a more complex behavior: they can form disordered aggregates, yield arrays of molecules with π–π stacking, or yield 5 × $\sqrt{3}$ surface structures.[17]

The reader can find a more detailed discussion on the most important surface techniques used for studying SAMs on Au(111) in ref 18.

There are some similarities and differences between thiol molecules adsorbed on Au(111) and on AuNPs. XPS characterization of thiol-capped AuNPs reveals that molecules are also attached to the AuNP surface by thiolate–Au bonds[1] (Figure 2b). However, the Au 4f and S 2p peaks slightly shift toward higher BE with respect to Au(111) for AuNP sizes < 4 nm (Figures 1 and 2).[19] The interpretation of these shifts is still unclear and could be attributed to different effects.[6] Also, chain ordering is affected by size effects since dodecanethiol-capped AuNPs with size < 2.8 nm exhibit a larger number of gauche defects than those found on Au(111).[19] The high radius of curvature and the high number of surface defects as the particle size decreases below 2–4 nm results in θ values higher than 0.33.[1,20] The presence of surface defects (at which thiolates are more strongly bonded) could explain the increased chemical stability against thiol degradation to disulfides and the reductive desorption behavior of SAMs on nanostructured Au and AuNPs compared with Au(111).[21]

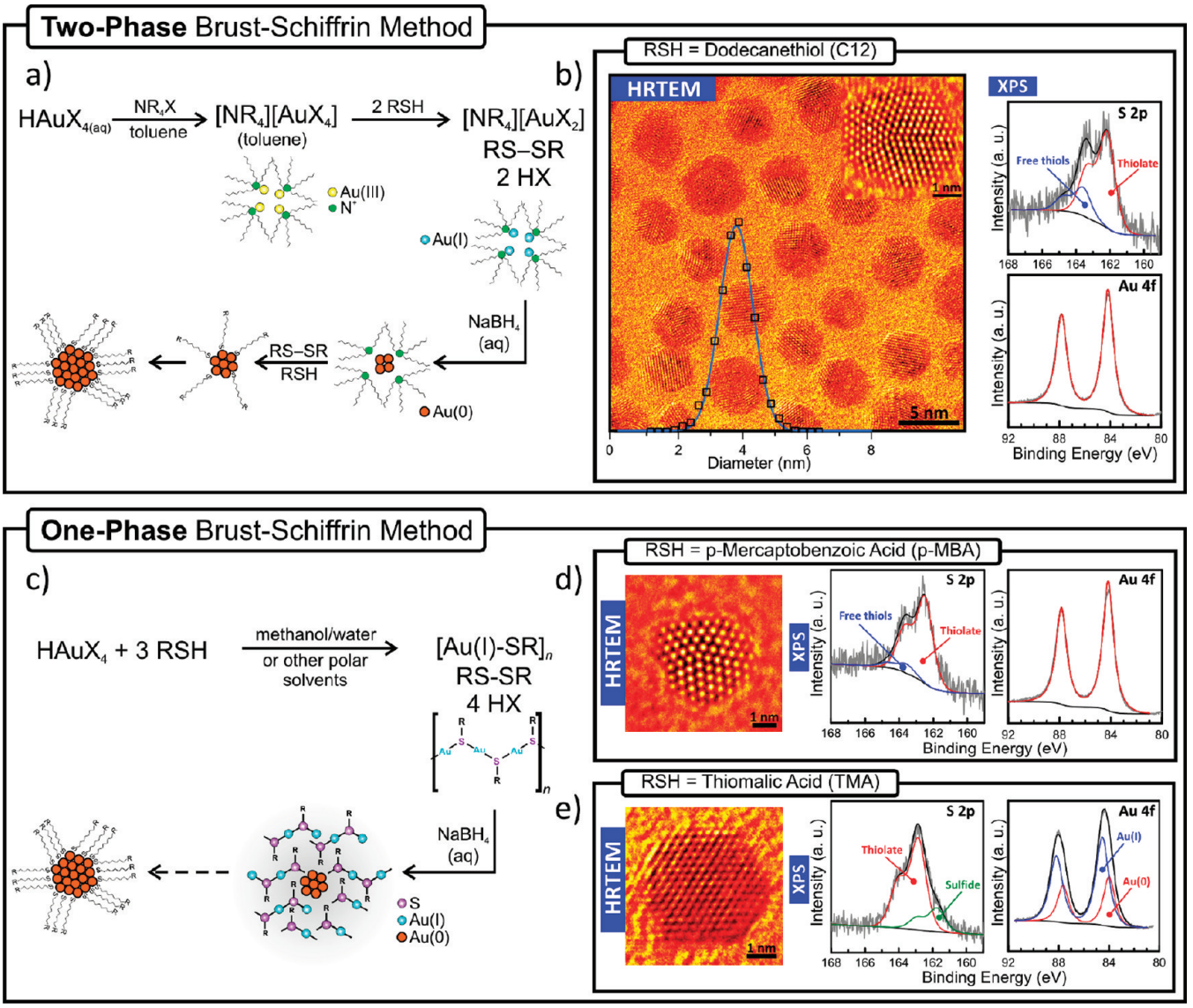

FIGURE 2. Schemes of the reactions involved in one- and two-phase Brust–Schiffrin methods. Some examples of AuNPs synthesized by both methods and their surface chemistry are included.

Therefore, it is evident that the thiol–gold interface has different physicochemical properties on small AuNPs and on Au(111). We will discuss this point in another section.

Preparation of Thiol SAMs on Au(111) and Synthesis of Thiol-Capped AuNPs

Thiol SAMs can be prepared by simple exposure of clean Au(111) surfaces to thiols (alkanethiols or arenethiols) or alkyldisulfides from both gas and liquid phases.[6] In gas phase, self-assembly initially involves the formation of the lying-down structures, which undergo a transition to the dense standing up $(\sqrt{3} \times \sqrt{3})$-R30° and c(4 × 2) lattices with increasing thiol exposure.[22] In self-assembly from liquid phase, the lying down phases are not observed and the system evolves directly to the $(\sqrt{3} \times \sqrt{3})$-R30° and c(4 × 2) lattices. However, it is possible to obtain the lying-down phases by controlled thiol desorption of dense lattices.[6]

The Brust–Schiffrin syntheses in one[23] and two phases[24] remain the preeminent methods to prepare hydrophilic and hydrophobic thiol-capped AuNPs, respectively, with a relatively high monodispersity and a mean size controllable by the thiol/Au(III) molar ratio (Figure 2).

In the two-phase method (II-PM), thiolate monolayer-protected AuNPs are obtained. First, Au(III) is transferred to a toluene phase using quaternary ammonium salts (NR_4X). Thiols, added to the organic phase, reduce Au(III) to Au(I) species. Although it was long believed that Au(I)–thiolate polymeric species ($[Au(I)–SR]_n$) were formed during this

reaction, recent experimental data have shown that ion pairs of tetraalkylammonium and Au(I)–halide complexes ($[NR_4][AuX_2]$) are the real precursors.[25] Au(I) species are encapsulated in an inverse micelle formed by the tetraalkylammonium, and after the addition of aqueous $NaBH_4$ solution, the metal reduction proceeds to the generation of Au(0) clusters. Then, thiol molecules dissolved in toluene bond to the cluster surface (Figure 2a).[26]

In the one-phase method (I-PM), Au(III) is first reduced to Au(I) upon addition of thiols in polar media (tetrahydrofuran, methanol), leading to the formation of $[Au(I)–SR]_n$, which are further reduced by $NaBH_4$ to obtain thiolate monolayer-protected AuNPs (Figure 2c). This is the case when, for instance, *p*-mercaptobenzoic acid (*p*-MBA) is used as the capping molecule (Figure 2d). However, in some conditions, $[Au(I)–SR]_n$ polymers are very stable in polar media, and incomplete reduction of these species can occur.[27] The existence of a $[Au(I)–SR]_n$ shell with ~1 nm Au(0) core has been reported for a typical I-PM reaction using thiomalic acid (TMA) (note the two components in the Au 4f XPS signal, Figure 2e).[28] The presence of $[Au(I)–TMA]_n$ can lead to misinterpretation of experimental data, because it is susceptible to being reduced under high-resolution transmission electron microscopy (HRTEM) imaging, resulting in larger AuNPs (~4 nm) (Figure 2e).[28] The assumption that $[Au(I)–SR]_n$ envelop Au cores can explain some intriguing data reported for NPs synthesized by I-PM. For instance, smaller Au–Au coordination numbers have been determined by extended X-ray absorption fine structure (EXAFS) for I-PM AuNPs (average size ~2.5 nm) compared with smaller (~2.1 nm) II-PM AuNPs.[29] Also, thermogravimetric analysis showed an extremely high organic content ($\theta = 0.89$), more than twice the value experimentally obtained[19] and theoretically predicted[20] for II-PM AuNPs of the same size.

Considering the differences in the mechanisms proposed for these methods, a more direct comparison between thiols adsorbed on planar Au and AuNPs should be made using AuNPs prepared by the II-PM,[24] where thiol molecules chemisorb directly on the Au(0) clusters,[26] forming the thiolate bond as on planar surfaces. However, subtle differences in the synthesis may greatly modify the mechanism. For instance, if the II-PM is carried out using a rather polar solvent (dichloromethane)[30] or some water is present in the reaction mixture,[26] $[Au(I)–SR]_n$ is formed.

The Chemistry of the S–Au Interface in Au Nanoclusters

The synthesis of extremely small thiol-capped AuNPs (diameter < 2 nm) leads to the formation of thermodynamically stable

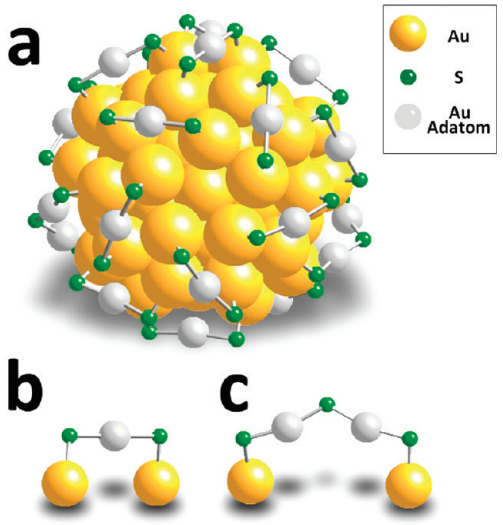

FIGURE 3. (a) $Au_{102}(p\text{-MBA})_{44}$ nanocluster. (b) The simple $RS–Au_{ad}–SR$ motif and (c) extended $RS–Au_{ad}–RS–Au_{ad}–SR$ motif. For clarity, R is not included. Adapted from M. A. MacDonald, X-ray Spectroscopic Studies of Gold–thiolate Nanoclusters, Dalhousie University, 2011.

clusters of the formula $Au_m(SR)_n$,[31] the properties of which differ from those of larger thiol-capped AuNPs. This is due to a different atomic packing symmetry and to the fact that their optical spectra are dominated by discrete single electron transitions between occupied and unoccupied electronic energy levels rather than by collective many-electron excitations.[32] Therefore, they are a link between larger thiol-capped AuNPs and inorganic complexes.

A key point in our present understanding of the surface chemistry of the S–Au interface has been the elucidation of the $Au_{102}(p\text{-MBA})_{44}$ crystal structure by X-ray diffraction.[33] The core of this thiolate-protected nanocluster (Figure 3), prepared by the I-PM, has been found to be packed in a Marks decahedron (79-atom Au core), surrounded by two types of "staple" motifs: $RS–Au_{ad}–SR$ and $RS–Au_{ad}–RS–Au_{ad}–SR$ (ad = adatom).[33]

Core sites contain a high Au–Au coordination number (10–12), while surface sites contain Au–S bonds as well as one Au–S bond anchoring the staple units to the cluster core. Staple sites have two Au–S bonds, as well as long-range "aurophilic" Au–S coordination between the staple Au and the cluster core. Au–S distances are 0.22–0.26 nm, while Au–S–Au and C–S–Au angles are 80–115° and 155–175°, respectively. Geometry optimization and ab initio molecular dynamics have shown that "staple" formation is preferred since it stabilizes the cluster by pinning the surface Au atoms.[34] Calculations for this nanocluster have shown the emergence of an energy gap of about 0.5 eV upon *p*-MBA adsorption.[35] As expected, the thiol coverage

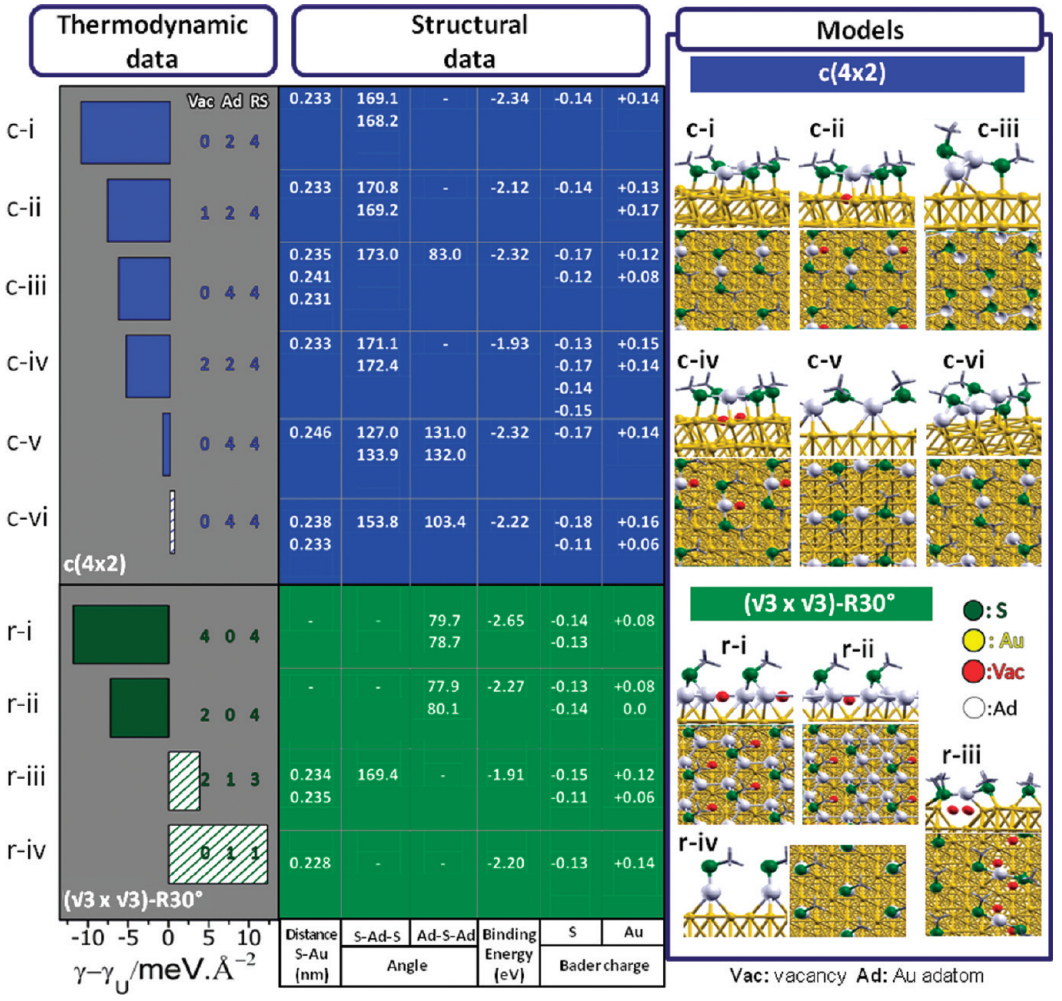

FIGURE 4. Optimized surfaces (top view and cross sections), thermodynamic and structural data for the different c(4 × 2) and (√3 × √3)-R30° models.

was $\theta = 0.7$, much higher than $\theta = 0.25$ for *p*-MBA on Au(111).[10] Also, the crystal structure of smaller thiol-capped nanoclusters prepared by the II-PM in a polar solvent is compatible with the extended staple motif.[30]

A recent study has analyzed the size-dependent nature of bonding in thiol-capped nanoclusters comparing $Au_{144}(SR)_{60}$, $Au_{38}(SR)_{24}$, and $Au_{25}(SR)_{18}$ (SR = PhC_2H_4S) clusters.[36] The d-electron depletion observed with the decrease in cluster size has been taken as proof of the existence of an increased fraction of "staples" as the metallic core becomes smaller.

The Chemistry of the S–Au Interface in Au(111)

Many efforts have been made to determine the adsorption site of the S head of the thiol molecules in the (√3 × √3)-R30° and c(4 × 2) lattices on Au(111) (Figure 1). Most of those studies considered an unreconstructed Au(111) surface (U), and hollow, bridge, or intermediate sites have been alternatively proposed as those energetically favored for chemisorption. However, these structural models have been contested since experimental data suggested that thiol chemisorption promotes a strong substrate reconstruction. Because chemical bonding is a local issue, one approach to tackle this problem is to use the information provided by Au nanoclusters. In this way, efforts have been recently made to model the thiolate–Au(111) interface in terms of RS–Au_{ad} species under the form of complexes or polymers, in analogy with those found in nanoclusters.[37–42] Eventually, a unified model for the thiol–Au interface with the RS–Au_{ad}–SR staple motif, valid for both Au nanoclusters and Au(111) surfaces, has been proposed.[43]

Despite the experimental evidence of the existence of RS–Au_{ad}–SR species in Au nanoclusters, this is not the case for SAMs on Au(111). Model-dependent surface analysis techniques have provided contradictory information for the dense phases,[44] and direct scanning tunneling microscopy (STM) has been achieved only at very low thiol coverage.[45] This difficulty to experimentally determine the exact nature of the interface has resulted in the development of different

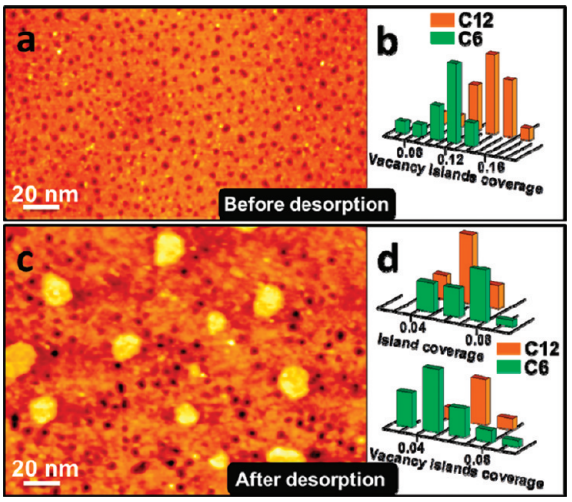

FIGURE 5. STM images of alkanethiol SAMs on Au(111) and related data (a, b) before and (c, d) after SAM electrochemical desorption. For experimental details, see ref 50.

models, most of them only based on density functional theory (DFT) calculations.

Modeling the Thiolate–Au(111) Interface

The chemistry and structural data of models containing RS–Au_{ad} units for the c(4 × 2) and ($\sqrt{3} \times \sqrt{3}$)-R30° thiolate-Au(111) interfaces and their thermodynamic stability in terms of the surface free energy (γ) are depicted in Figure 4. The S–Au distances and Au_{ad}–S–Au_{ad} angles for the c(4 × 2) lattice are in good agreement with those reported for the RS–Au_{ad}–SR staple found in Au_{102}(*p*-MBA)$_{44}$ nanoclusters, thus supporting the unified model.[33] The thermodynamic data in Figure 4 show that models with a 1:2 Au_{ad}/RS ratio (c-i, c-ii, c-iv), are energetically preferred compared with both thiol adsorbed on U and 1:1 Au_{ad}/thiol ratio models (c-iii, c-v, c-vi).[41] In particular, the c-i model, which contains the staple motif (RS–Au_{ad}–SR), is extremely stable because each S atom is bonded not only to one Au adatom but also to another Au surface atom, resulting in a large binding energy. Also, this surface structure involves a smaller number of Au_{ad} than 1:1 Au_{ad}/RS ratio models, thus requiring a smaller amount of formation energy. New models containing the staple motif either with an isolated vacancy (c-ii)[46,47] or with two isolated vacancies (c-iv) in the unit cell have been recently reported, although they are more unstable because of the extra energy needed to form vacancies. Clearly, although γ values favor staple motif models (Figure 4),[6,48] these are not consistent with the experimentally observed ($\sqrt{3} \times \sqrt{3}$)-R30° lattice (Figure 1) and require either RS–Au_{ad} (r-iv) or RS–Au_{ad}–SR + RS–Au(111) species (r-iii), which are unstable with respect to U (Figure 4). A ($\sqrt{3} \times \sqrt{3}$)-R30° lattice with good stability can be obtained for models containing only vacancies (r-i, r-ii).[49]

Experimental Evidence on Thiolate–Au Interfacial Chemistry

A possible sign of Au adatom uptake from the Au(111) surface to form the RS–Au_{ad} moieties are serrated edge steps and vacancy islands observed by STM (Figure 5a). The vacancy island coverage (θ_{vac}) on large terraces, where the probability of step edge contribution to Au_{ad} formation is small, would give information on the nature of the RS–Au_{ad} species. Indeed, for thiol SAMs with $\theta = 0.33$, such as in ($\sqrt{3} \times \sqrt{3}$)-R30° or c(4 × 2) lattices, formation of RS–Au_{ad} or RS–Au_{ad}–SR moieties requires $\theta_{vac} = 0.33$ and $\theta_{vac} = 0.165$, respectively.[6] The most probable θ_{vac} values found for SAMs of hexanethiol (C6) and dodecanethiol (C12) are 0.12 and 0.14, respectively (Figure 5b),[50] close to that expected for RS–Au_{ad}–SR moieties and incompatible with RS–Au_{ad} or $(RSAu)_x$ species. A decrease in θ_{vac} in going from methanethiol ($\theta_{vac} = 0.12/0.20$) to butanethiol ($\theta_{vac} = 0.04$) SAMs has been reported, suggesting ligand-dependent reduction of vacancy mobility.[47,51] However, our data show higher θ_{vac} values for longer thiols (Figure 5b).

In the frame of the adatom models, thiol desorption from RS–Au_{ad} or RS–Au_{ad}–SR moieties at large terraces should lead to the nucleation and growth of two-dimensional Au islands from the released Au_{ad} (Figure 5c). Therefore, the surface coverage of these islands (θ_{isl}) on Au(111) terraces, where adatoms cannot be trapped by steps, provide information about the thiol species present on the Au surface before desorption. However, the mobile Au_{ad} can fill the vacancy islands, so that quantitative information requires not only the estimation of θ_{isl} (Figure 5d) but also the estimation of θ_{vac} after desorption (θ_{vacf}) (Figure 5d).[50] Then, the total coverage by Au adatoms after desorption is $\theta_{ad} = \theta_{isl} + (\theta_{vac} - \theta_{vacf})$.

The analysis of C6 and C12 data yields $\theta_{ad} = 0.12$ and 0.14, respectively, consistent with the RS–Au_{ad}–SR motif. However, in C12 SAMs the ($\sqrt{3} \times \sqrt{3}$)-R30° is the predominant lattice, which is incompatible with a plain staple model. Also, the experimentally observed $\theta_{ad} = 0.14$ cannot be explained by simple vacancy models (r-i, r-ii) because they do not contain RS–Au_{ad} species (Figure 4). Obtained θ_{ad} values agree with those reported in ref 52 for hydrogen-induced thiol desorption. These results contrast with $\theta_{ad} = 0.22$ reported in ref 53 for thiol desorption produced by water electrolysis assisted by STM tips. High θ_{ad} values (~0.4) were also observed by in situ STM

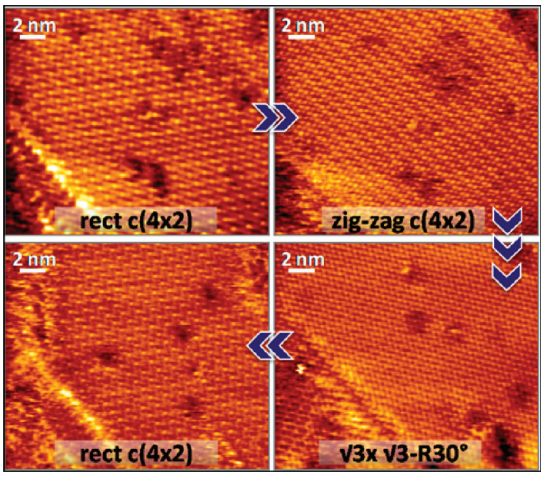

FIGURE 6. Consecutive STM images of a C6 SAM on Au(111) showing reversible c(4 × 2) ⇔ (√3 × √3)-R30° transitions for constant imaging conditions. Note also some pinhole and defect fluctuation. See ref 54 for experimental details.

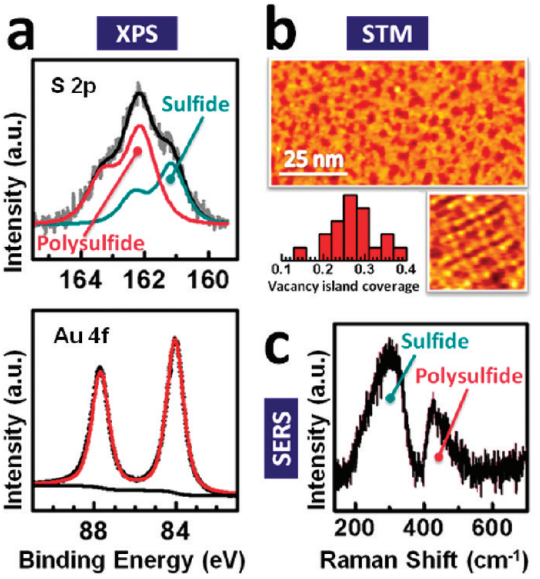

FIGURE 7. Surface characterization of sulfur on gold. All SAMs were formed from sulfide solutions.

during SAM reductive electrodesorption.[6] While θ_{ad} = 0.22/0.40 seems to favor RS–Au_{ad} models (θ_{ad} = 0.33), the cross-section analysis of the islands suggests that they could actually include thiol aggregates, thus overestimating θ_{ad}.[6,53]

Some aromatic thiols exhibit an "anomalous" behavior: Au islands of monatomic height with θ_{isl} = 0.5 are formed instead of the vacancy islands observed for aliphatic thiols.[11,16] Yet a different behavior has been reported for 6-mercaptopurine SAMs on Au(111), where there is no evidence either of vacancy islands or of a significant amount of Au islands.[50] How the staple model could be consistent with the large θ_{isl} values observed for some aromatic thiols or with the θ_{vac} = 0 found for N-heterocyclic thiols remains to be answered.

A Possible Pathway for c(4 × 2) Formation

A possible pathway for the formation of the c(4 × 2) lattice starting from the U surface has been suggested.[46] After thiol physisorption at on-top positions in the U surface and S–H bond scission, the chemisorbed radicals would move toward the most stable bridge-fcc positions forming the (√3 × √3)-R30° lattice. Afterward, the chemisorbed RS species would take adatoms from the Au surface, leading to the c(4 × 2) lattice containing RS–Au_{ad}–SR and single-atom vacancies (models c-ii and c-iv). Finally, the system would lower its surface free energy by annihilation of the single atom vacancies that incorporate at step edges or form vacancy islands. This energetically favored pathway (c-iv/c-ii → c-i, see Figure 4, left) can explain the presence of (√3 × √3)-R30° and c(4 × 2) domains (Figure 1a) and also the vacancy islands (Figure 5a) observed for most thiol SAMs.[46] On the other hand, thiol desorption from the staples originates free Au adatoms that form the observed Au islands (Figure 5c).

In this scenario, the (√3 × √3)-R30° lattice, predominantly found for intermediate or long alkanethiols, like C12, can be explained by the larger intermolecular forces, which would "freeze" the U surface[14] hindering the reconstruction. The somewhat unstable r-iii (√3 × √3)-R30° model, which contains a thiol molecule at a bridge position and also the "staple" and vacancies (Figure 4, models), can connect the U surface with the staple models. This could explain the c(4 × 2) ⇔ (√3 × √3)-R30° transformations observed in real time (Figure 6). However, the thermodynamically stable vacancy models for the (√3 × √3)-R30° lattice (r-i, r-ii) are not feasible since they cannot explain the Au adatom islands observed after thiol desorption in the cases where the (√3 × √3)-R30° lattice is predominant, like C12.

The Chemistry of the Sulfur–Au Interface

This system is important since SAMs of short thiols on Au(111) and AuNPs usually contain a variable amount of sulfides.[28,55,56] Sulfur adsorbs on Au(111) forming a covalent bond and different structures, depending on the surface coverage.[57] At low coverage a (√3 × √3)-R30° lattice (θ = 0.33) is formed, similar to what is observed in thiolate SAMs, characterized by a S 2p XPS signal at 161.5 eV (Figure 7a). At higher coverage, other structures, such as S trimers (S_3) and rectangles (S_8) (Figure 7b), are observed by STM, which have been assigned either to adsorbed polysulfides (S 2p signal at 162.3 eV) (Figure 7a)[57] or to an

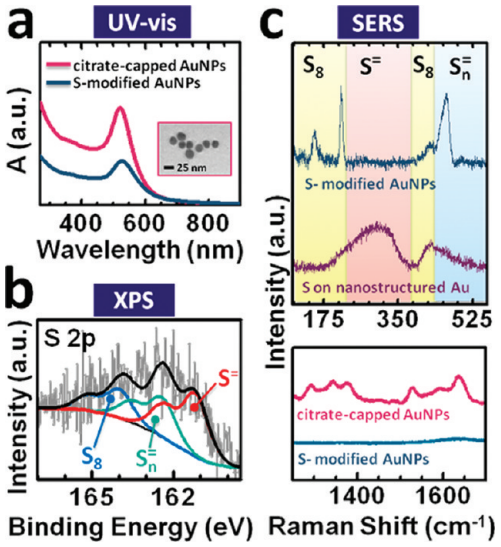

FIGURE 8. Surface characterization of S modified Au nanoparticles.

ordered AuS phase produced by Au corrosion.[58] Also, S adsorption is accompanied by the formation of vacancy islands ($\theta_{vac} \approx 0.25$) (Figure 7b) that have been associated with the Au corrosion process.

Although it has been proposed that this AuS phase consists of S atoms bonded to oxidized Au species,[58] these cannot be observed in the XP spectra (Figure 7a). Surface-enhanced Raman spectroscopy (SERS) data of nanostructured gold samples after immersion in the sulfide-containing electrolyte,[57] whose XP spectra have the same species as those on Au(111), show bands at ~315 cm^{-1} (S–Au stretching in monomeric S) and ~450 cm^{-1} (S–S stretching in adsorbed polysulfide species on Au)[57] (Figure 7c). This would indicate that the interface cannot be described in terms of a simple and ordered AuS layer. Also, new STM data confirm that the rectangular species shown in Figure 7b correspond to S_8.[59]

The Controversy of the Sulfur–Gold Interface in Nanoparticles

The S–Au interface in AuNPs is also under continuous discussion because of their potential use in nanomedicine and metal ion-sensors. In the simplest case, AuNPs have been exposed to H_2S or to Na_2S solutions,[60] and the resulting interface was described as a gold sulfide. However, citrate-capped AuNPs (Figure 8a, inset) treated with sulfide and purified by dialysis show a more complex S–Au interface. The AuNPs do not aggregate (Figure 8a), and there is complete displacement of citrate ions by S species (Figure 8c). XPS data show three S 2p components (sulfide, polysulfides and elemental S, Figure 8b), while the Au 4f region shows no evidence of oxidized species (data not shown). SER spectra also indicate that the main species are adsorbed polysulfides and elemental sulfur (Figure 8c).

As in the synthesis of thiol-capped AuNPs, the mixing of Au(III) salts with a sulfur-containing reactant results in nanoparticles with a complex chemistry. In fact, depending on the authors, the reaction of sulfide with gold salts yields NPs with a gold sulfide core and a gold shell (together with small AuNPs)[61,62] or AuNP aggregates, nanorods, or nanoplates.[63,64] Therefore, more research is needed to clarify the nature of the S species present on the AuNPs surfaces and its dependence on the synthesis route.

Concluding Remarks

Recent relevant experimental and theoretical evidence on the chemistry and structure of the S–Au interface, both for planar and for nanoparticle surfaces, have been critically reviewed under the light of a unified model. Present models are mostly based on the chemistry and structure of gold nanoclusters, where the "staple" motifs have been detected. However, the fact that the RS–Au_{ad}–SR staples have been clearly detected only for AuNPs that yield these as intermediate synthesis products opens the question about the validity of this model for nanoparticles prepared by other methods and for planar surfaces at high thiol coverage. In the latter case, the "staple" models, which can only be applied to low coverage and c(4 × 2) lattices, reasonably explains the Au vacancy and Au adatom islands present on the Au(111) surface. Intriguing points, which cannot be yet rationalized in terms of this model, include the structure of the ($\sqrt{3} \times \sqrt{3}$)-R30° lattice, the mechanism of ($\sqrt{3} \times \sqrt{3}$)-R30° ⇔ c(4 × 2) transformations, the origin of the Au islands (or vacancies) for aromatic thiols, and the absence of vacancy islands for N-heterocyclic thiols. Finally, an accurate picture of the sulfur–Au interface and how this can be incorporated in the context of the present scenario remains unclear.

We acknowledge support from ANPCyT (Argentina, PICT-2010-2554, PICT-2010-0423), CONICET (Argentina, PIP 11220090100139), MICINN (Spain, CTQ2008-06017/BQU), ACIISI (Canarias, ID20100152), NCEM-Lawrence Berkeley Lab, Optics Laboratory-Instituto Balseiro, Fulbright and Bunge y Born Foundation. We thank J. Azcárate for the synthesis of II-PM AuNPs, and G. Andreasen for some STM images.

BIOGRAPHICAL INFORMATION

Evangelina Pensa is a CONICET Ph.D. Fellow at the Research Institute of Theoretical and Applied Physical Chemistry (INIFTA). She received her degree in Chemistry (2009) from the National University of La Plata (UNLP).

Emiliano Cortés is a CONICET Ph.D. Fellow at INIFTA. He received his degree in Chemistry (2008) from UNLP.

Gastón Corthey is a Doctoral Fellow of the Swiss National Science Foundation at INIFTA. He received his degree in Chemistry (2008) from UNLP.

Pilar Carro received her Ph.D. from La Laguna University (ULL), Spain (1986). She is Professor of Physical Chemistry at ULL.

Carolina Vericat received her Ph.D. from UNLP (2003). She is Assistant Researcher of CONICET at INIFTA and Professor of Chemistry at UNLP.

Mariano H. Fonticelli received his Ph.D. from UNLP (2002). He is Assistant Researcher of CONICET at INIFTA and Professor of Chemistry at UNLP.

Guillermo Benitez received his Ph.D. from UNLP (2001). He is Assistant Researcher of CONICET at INIFTA.

Aldo A. Rubert received his Ph.D. from UNLP (2008). He is Researcher of UNLP at INIFTA.

Roberto C. Salvarezza received his Ph.D. from the University of Buenos Aires, Argentina (1981). He is Superior Researcher of CONICET and Director of INIFTA.

FOOTNOTES

*To whom correspondence should be addressed. E-mail: robsalva@inifta.unlp.edu.ar.
The authors declare no competing financial interest.

REFERENCES

1 Love, J. C.; Estroff, L. A.; Kriebel, J. K.; Nuzzo, R. G.; Whitesides, G. M. Self-assembled monolayers of thiolates on metals as a form of nanotechnology. *Chem. Rev.* **2005**, *105*, 1103–1170.

2 Boisselier, E.; Astruc, D. Gold nanoparticles in nanomedicine: Preparations, imaging, diagnostics, therapies and toxicity. *Chem. Soc. Rev.* **2009**, *38*, 1759–1782.

3 Gobin, A. M.; Watkins, E. M.; Quevedo, E.; Colvin, V. L.; West, J. L. Near-infrared-resonant gold/gold sulfide nanoparticles as a photothermal cancer therapeutic agent. *Small* **2010**, *6*, 745–752.

4 Sardar, R.; Funston, A. M.; Mulvaney, P.; Murray, R. W. Gold nanoparticles: Past, present, and future. *Langmuir* **2009**, *25*, 13840–13851.

5 Vericat, C.; Vela, M. E.; Salvarezza, R. C. Self-assembled monolayers of alkanethiols on Au(111): Surface structures, defects and dynamics. *Phys. Chem. Chem. Phys.* **2005**, *7*, 3258–3268.

6 Vericat, C.; Vela, M. E.; Benitez, G.; Carro, P.; Salvarezza, R. C. Self-assembled monolayers of thiols and dithiols on gold: New challenges for a well-known system. *Chem. Soc. Rev.* **2010**, *39*, 1805–1834.

7 Zhang, J.; Bilic, A.; Reimers, J. R.; Hush, N. S.; Ulstrup, J. Coexistence of multiple conformations in cysteamine monolayers on Au(111). *J. Phys. Chem. B* **2005**, *109*, 15355–15367.

8 Zhou; Baunach, T.; Ivanova, V.; Kolb, D. M. Structure and electrochemistry of 4,4′-dithiodipyridine self-assembled monolayers in comparison with 4-mercaptopyridine self-assembled monolayers on Au(111). *Langmuir* **2004**, *20*, 4590–4595.

9 Yang, G.; Liu, G.-y. New insights for self-assembled monolayers of organothiols on Au(111) revealed by scanning tunneling microscopy. *J. Phys. Chem. B* **2003**, *107*, 8746–8759.

10 Urcuyo, R.; Cortés, E.; Rubert, A. A.; Benitez, G.; Montero, M. L.; Tognalli, N. G.; Fainstein, A.; Vela, M. E.; Salvarezza, R. C. Aromatic and aliphatic thiol self-assembled monolayers on Au: Anchoring and delivering copper species. *J. Phys. Chem. C* **2011**, *115*, 24707–24717.

11 Jin, Q.; Rodriguez, J. A.; Li, C. Z.; Darici, Y.; Tao, N. J. Self-assembly of aromatic thiols on Au(111). *Surf. Sci.* **1999**, *425*, 101–111.

12 Grumelli, D.; Méndez De Leo, L. P.; Bonazzola, C.; Zamlynny, V.; Calvo, E. J.; Salvarezza, R. C. Methylene blue incorporation into alkanethiol SAMs on Au(111): Effect of hydrocarbon chain ordering. *Langmuir* **2010**, *26*, 8226–8232.

13 Torrelles, X.; Barrena, E.; Munuera, C.; Rius, J.; Ferrer, S.; Ocal, C. New insights in the c(4 × 2) reconstruction of hexadecanethiol on Au(111) revealed by grazing incidence X-ray diffraction. *Langmuir* **2004**, *20*, 9396–9402.

14 Torrelles, X.; Vericat, C.; Vela, M. E.; Fonticelli, M. H.; Daza Millone, M. A.; Felici, R.; Lee, T.-L.; Zegenhagen, J.; Muñoz, G.; Martín-Gago, J. A.; Salvarezza, R. C. Two-site adsorption model for the ($\sqrt{3}\times\sqrt{3}$)-R30° dodecanethiolate lattice on Au(111) surfaces. *J. Phys. Chem. B* **2006**, *110*, 5586–5594.

15 Dhirani, A.-A.; Zehner, R. W.; Hsung, R. P.; Guyot-Sionnest, P.; Sita, L. R. Self-assembly of conjugated molecular rods: A high-resolution STM study. *J. Am. Chem. Soc.* **1996**, *118*, 3319–3320.

16 Duan, L.; Garrett, S. J. An investigation of rigid p-methylterphenyl thiol self-assembled monolayers on Au(111) using reflection-absorption infrared spectroscopy and scanning tunneling microscopy. *J. Phys. Chem. B* **2001**, *105*, 9812–9816.

17 Xu, Q.; Ma, H.; Yip, H.; Jen, A. K.-Y. Controlled assembly of large π-conjugated aromatic thiols on Au(111). *Nanotechnology* **2008**, *19*, No. 135605.

18 Vericat, C.; Vela, M. E.; Benitez, G.; Martin-Gago, J. A.; Torrelles, X.; Salvarezza, R. C. Surface characterization of sulfur and alkanethiol self-assembled monolayers on Au(111). *J. Phys.: Condens. Matter* **2006**, *18*, No. R867.

19 Hostetler, M. J.; Wingate, J. E.; Zhong, C.-J.; Harris, J. E.; Vachet, R. W.; Clark, M. R.; Londono, J. D.; Green, S. J.; Stokes, J. J.; Wignall, G. D.; Glish, G. L.; Porter, M. D.; Evans, N. D.; Murray, R. W. Alkanethiolate gold cluster molecules with core diameters from 1.5 to 5.2 nm: Core and monolayer properties as a function of core size. *Langmuir* **1998**, *14*, 17–30.

20 Olmos-Asar, J. A.; Rapallo, A.; Mariscal, M. M. Development of a semiempirical potential for simulations of thiol-gold interfaces. Application to thiol-protected gold nanoparticles. *Phys. Chem. Chem. Phys.* **2011**, *13*, 6500–6506.

21 Vericat, C.; Benitez, G. A.; Grumelli, D. E.; Vela, M. E.; Salvarezza, R. C. Thiol-capped gold: From planar to irregular surfaces. *J. Phys.: Condens. Matter* **2008**, *20*, No. 184004.

22 Poirier, G. E.; Pylant, E. D. The self-assembly mechanism of alkanethiols on Au(111). *Science* **1996**, *272*, 1145–1148.

23 Brust, M.; Fink, J.; Bethell, D.; Schiffrin, D. J.; Kiely, C. Synthesis and reactions of functionalised gold nanoparticles. *J. Chem. Soc., Chem. Commun.* **1995**, 1655–1656.

24 Brust, M.; Walker, M.; Bethell, D.; Schiffrin, D. J.; Whyman, R. Synthesis of thiol-derivatised gold nanoparticles in a two-phase liquid-liquid system. *J. Chem. Soc., Chem. Commun.* **1994**, 801–802.

25 Goulet, P. J. G.; Lennox, R. B. New insights into Brust–Schiffrin metal nanoparticle synthesis. *J. Am. Chem. Soc.* **2010**, *132*, 9582–9584.

26 Li, Y.; Zaluzhna, O.; Xu, B.; Gao, Y.; Modest, J. M.; Tong, Y. J. Mechanistic insights into the Brust–Schiffrin two-phase synthesis of organo-chalcogenate-protected metal nanoparticles. *J. Am. Chem. Soc.* **2011**, *133*, 2092–2095.

27 Ackerson, C. J.; Jadzinsky, P. D.; Kornberg, R. D. Thiolate ligands for synthesis of water-soluble gold clusters. *J. Am. Chem. Soc.* **2005**, *127*, 6550–6551.

28 Corthey, G.; Giovanetti, L. J.; Ramallo-López, J. M.; Zelaya, E.; Rubert, A. A.; Benitez, G. A.; Requejo, F. G.; Fonticelli, M. H.; Salvarezza, R. C. Synthesis and characterization of gold@gold(I)-thiomalate core@shell nanoparticles. *ACS Nano* **2010**, *4*, 3413–3421.

29 Sun, Y.; Frenkel, A. I.; White, H.; Zhang, L.; Zhu, Y.; Xu, H.; Yang, J. C.; Koga, T.; Zaitsev, V.; Rafailovich, M. H.; Sokolov, J. C. Comparison of decanethiolate gold nanoparticles synthesized by one-phase and two-phase methods. *J. Phys. Chem. B* **2006**, *110*, 23022–23030.

30 Heaven, M. W.; Dass, A.; White, P. S.; Holt, K. M.; Murray, R. W. Crystal structure of the gold nanoparticle $[N(C_8H_{17})_4][Au_{25}(SCH_2CH_2Ph)_{18}]$. *J. Am. Chem. Soc.* **2008**, *130*, 3754–3755.

31 Schaaff, T. G.; Shafigullin, M. N.; Khoury, J. T.; Vezmar, I.; Whetten, R. L. Properties of a ubiquitous 29 kDa Au:SR cluster compound. *J. Phys. Chem. B* **2001**, *105*, 8785–8796.

32 Zhu, M.; Aikens, C. M.; Hollander, F. J.; Schatz, G. C.; Jin, R. Correlating the crystal structure of a thiol-protected Au_{25} cluster and optical properties. *J. Am. Chem. Soc.* **2008**, *130*, 5883–5885.

33 Jadzinsky, P. D.; Calero, G.; Ackerson, C. J.; Bushnell, D. A.; Kornberg, R. D. Structure of a thiol monolayer-protected gold nanoparticle at 1.1 Å resolution. *Science* **2007**, *318*, 430–433.

34 Jiang, D.-e.; Tiago, M. L.; Luo, W.; Dai, S. The "staple" motif: A key to stability of thiolate-protected gold nanoclusters. *J. Am. Chem. Soc.* **2008**, *130*, 2777–2779.

35 Li, Y.; Galli, G.; Gygi, F. Electronic structure of thiolate-covered gold nanoparticles: $Au_{102}(MBA)_{44}$. *ACS Nano* **2008**, *2*, 1896–1902.

36 MacDonald, M. A.; Zhang, P.; Qian, H.; Jin, R. Site-specific and size-dependent bonding of compositionally precise gold-thiolate nanoparticles from X-ray spectroscopy. *J. Phys. Chem. Lett.* **2010**, *1*, 1821–1825.

37 Mazzarello, R.; Cossaro, A.; Verdini, A.; Rousseau, R.; Casalis, L.; Danisman, M. F.; Floreano, L.; Scandolo, S.; Morgante, A.; Scoles, G. Structure of a CH_3S monolayer on Au(111) solved by the interplay between Molecular Dynamics calculations and diffraction measurements. *Phys. Rev. Lett.* **2007**, *98*, No. 016102.

38 Cossaro, A.; Mazzarello, R.; Rousseau, R.; Casalis, L.; Verdini, A.; Kohlmeyer, A.; Floreano, L.; Scandolo, S.; Morgante, A.; Klein, M. L.; Scoles, G. X-ray diffraction and computation yield the structure of alkanethiols on gold(111). *Science* **2008**, *321*, 943–946.

39 Grönbeck, H.; Häkkinen, H. Polymerization at the alkylthiolate-Au(111) interface. *J. Phys. Chem. B* **2007**, *111*, 3325–3327.

40 Häkkinen, H.; Walter, M.; Grönbeck, H. Divide and protect: Capping gold nanoclusters with molecular gold-thiolate rings. *J. Phys. Chem. B* **2006**, *110*, 9927–9931.

41 Grönbeck, H.; Häkkinen, H.; Whetten, R. L. Gold-thiolate complexes form a unique c(4 × 2) structure on Au(111). *J. Phys. Chem. C* **2008**, *112*, 15940–15942.

42 Jiang, D.-e.; Dai, S. Constructing gold-thiolate oligomers and polymers on Au(111) based on the linear S-Au-S geometry. *J. Phys. Chem. C* **2009**, *113*, 7838–7842.

43 Walter, M.; Akola, J.; Lopez-Acevedo, O.; Jadzinsky, P. D.; Calero, G.; Ackerson, C. J.; Whetten, R. L.; Grönbeck, H.; Häkkinen, H. A unified view of ligand-protected gold clusters as superatom complexes. *Proc. Natl. Acad. Sci. U.S.A.* **2008**, *105*, 9157–9162.

44 Sheppard, D. C.; Parkinson, G. S.; Hentz, A.; Window, A. J.; Quinn, P. D.; Woodruff, D. P.; Bailey, P.; Noakes, T. C. Q. Medium energy ion scattering investigation of methylthiolate-induced modification of the Au(111) surface. *Surf. Sci.* **2011**, *605*, 138–145.

45 Maksymovych, P.; Sorescu, D. C.; Yates, J. T., Jr. Gold-adatom-mediated bonding in self-assembled short-chain alkanethiolate species on the Au(111) Surface. *Phys. Rev. Lett.* **2006**, *97*, No. 146103.

46 Torres, E.; Blumenau, A. T.; Biedermann, P. U. Mechanism for phase transitions and vacancy island formation in alkylthiol/Au(111) self-assembled monolayers based on adatom and vacancy-induced reconstructions. *Phys. Rev. B* **2009**, *79*, No. 075440.

47 Wang, Y.; Chi, Q.; Hush, N. S.; Reimers, J. R.; Zhang, J.; Ulstrup, J. Scanning tunneling microscopic observation of adatom-mediated motifs on gold-thiol self-assembled monolayers at high coverage. *J. Phys. Chem. C* **2009**, *113*, 19601–19608.

48 Carro, P.; Salvarezza, R.; Torres, D.; Illas, F. On the thermodynamic stability of ($\sqrt{3}\times\sqrt{3}$)-R30° methanethiolate lattice on reconstructed Au(111) surface models. *J. Phys. Chem. C* **2008**, *112*, 19121–19124.

49 Molina, L. M.; Hammer, B. Theoretical study of thiol-induced reconstructions on the Au(111) surface. *Chem. Phys. Lett.* **2002**, *360*, 264–271.

50 Pensa, E.; Carro, P.; Rubert, A. A.; Benítez, G.; Vericat, C.; Salvarezza, R. C. Thiol with an unusual adsorption-desorption behavior: 6-Mercaptopurine on Au(111). *Langmuir* **2010**, *26*, 17068–17074.

51 Wang, Y.; Chi, Q.; Hush, N. S.; Reimers, J. R.; Zhang, J.; Ulstrup, J. Gold mining by alkanethiol radicals: Vacancies and pits in the self-assembled monolayers of 1-propanethiol and 1-butanethiol on Au(111). *J. Phys. Chem. C* **2011**, *115*, 10630–10639.

52 Kautz, N. A.; Kandel, S. A. Alkanethiol monolayers contain gold adatoms, and adatom coverage is independent of chain length. *J. Phys. Chem. C* **2009**, *113*, 19286–19291.

53 Li, F.-S.; Zhou, W.; Guo, Q. Uncovering the hidden gold atoms in a self-assembled monolayer of alkanethiol molecules on Au(111). *Phys. Rev. B* **2009**, *79*, No. 113412.

54 Vericat, C.; Andreasen, G.; Vela, M. E.; Martin, H.; Salvarezza, R. C. Following transformation in self-assembled alkanethiol monolayers on Au(111) by in situ scanning tunneling microscopy. *J. Chem. Phys.* **2001**, *115*, 6672–6678.

55 Sawaguchi, T.; Mizutani, F.; Yoshimoto, S.; Taniguchi, I. Voltammetric and in situ STM studies on self-assembled monolayers of 4-mercaptopyridine, 2-mercaptopyridine and thiophenol on Au(111) electrodes. *Electrochim. Acta* **2000**, *45*, 2861–2867.

56 Cometto, F. P.; Macagno, V. A.; Paredes-Olivera, P.; Patrito, E. M.; Ascolani, H.; Zampieri, G. Decomposition of methylthiolate monolayers on Au(111) prepared from dimethyl disulfide in solution phase. *J. Phys. Chem. C* **2010**, *114*, 10183–10194.

57 Lustemberg, P. G.; Vericat, C.; Benitez, G. A.; Vela, M. E.; Tognalli, N.; Fainstein, A.; Martiarena, M. L.; Salvarezza, R. C. Spontaneously formed sulfur adlayers on gold in electrolyte solutions: Adsorbed sulfur or gold sulfide? *J. Phys. Chem. C* **2008**, *112*, 11394–11402.

58 Biener, M. M.; Biener, J.; Friend, C. M. Revisiting the S-Au(111) interaction: Static or dynamic? *Langmuir* **2005**, *21*, 1668–1671.

59 Koczkur, K. M.; Hamed, E. M.; Houmam, A. Sulfur multilayer formation on Au(111): New insights from the study of hexamethyldisilathiane. *Langmuir* **2011**, *27*, 12270–12274.

60 Fan, Y.; Long, Y. F.; Li, Y. F. A sensitive resonance light scattering spectrometry of trace Hg^{2+} with sulfur ion modified gold nanoparticles. *Anal. Chim. Acta* **2009**, *653*, 207–211.

61 Averitt, R. D.; Sarkar, D.; Halas, N. J. Plasmon resonance shifts of Au-coated Au_2S nanoshells: Insight into multicomponent nanoparticle growth. *Phys. Rev. Lett.* **1997**, *78*, 4217–4220.

62 Raschke, G.; Brogl, S.; Susha, A. S.; Rogach, A. L.; Klar, T. A.; Feldmann, J.; Fieres, B.; Petkov, N.; Bein, T.; Nichtl, A.; Kürzinger, K. Gold nanoshells improve single nanoparticle molecular sensors. *Nano Lett.* **2004**, *4*, 1853–1857.

63 Schwartzberg, A. M.; Grant, C. D.; van Buuren, T.; Zhang, J. Z. Reduction of $HAuCl_4$ by Na_2S revisited: The case for Au nanoparticle aggregates and against Au_2S/Au core/shell particles. *J. Phys. Chem. C* **2007**, *111*, 8892–8901.

64 Mikhlin, Y.; Likhatski, M.; Karacharov, A.; Zaikovski, V.; Krylov, A. Formation of gold and gold sulfide nanoparticles and mesoscale intermediate structures in the reactions of aqueous $HAuCl_4$ with sulfide and citrate ions. *Phys. Chem. Chem. Phys.* **2009**, *11*, 5445–5454.